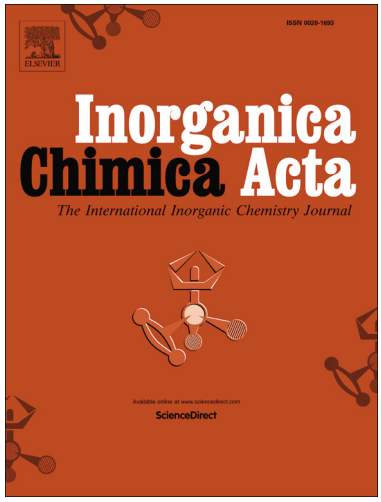

Nucleus targeting anthraquinone-based copper (II) complexes as the potent PDT agents: Synthesis, photo-physical and theoretical evaluation

Longjam Reena Devi, Md Kausar Raza, Dulal Musib, Vanitha Ramu, Joshila Devi, Mithun Roy

PII: S0020-1693(19)30969-7
DOI: https://doi.org/10.1016/j.ica.2019.119208
Reference: ICA 119208

To appear in: *Inorganica Chimica Acta*

Received Date: 3 July 2019
Revised Date: 4 September 2019
Accepted Date: 14 October 2019

Please cite this article as: L.R. Devi, M.K. Raza, D. Musib, V. Ramu, J. Devi, M. Roy, Nucleus targeting anthraquinone-based copper (II) complexes as the potent PDT agents: Synthesis, photo-physical and theoretical evaluation, *Inorganica Chimica Acta* (2019), doi: https://doi.org/10.1016/j.ica.2019.119208

Nucleus targeting anthraquinone-based copper (II) complexes as the potent PDT agents: Synthesis, photo-physical and theoretical evaluation

Longjam Reena Devi,[†] Md Kausar Raza[‡], Dulal Musib,[†] Vanitha Ramu[‡], Joshila Devi[†] and Mithun Roy[*,†]

†Department of Chemistry, National Institute of Technology, Manipur, Langol 795004, Imphal (Manipur), India

‡Department of Inorganic and Physical Chemistry, Indian Institute of Science, Bangalore 560012 (India)

Keywords: Copper(II) complexes, nuclear localization, photodynamic therapy, ROS generation, apoptosis.

Highlights:

- *In vitro* photodynamic activity of anthraquinone-based copper(II) complexes is reported here.
- Increased concentration of singlet oxygen ($^1O_2$) generated from type-II photo-process was responsible for the photocytotoxicity through apoptosis.
- Generation of $^1O_2$ by the photo-activated copper(II) complexes was evaluated photo-physically and theoretically.

---

*Author to whom correspondence should be addressed. E-mail: mithunroy@nitmanipur.ac.in, mithunroy.iisc@gmail.com

Abstract: Present work explored the structural aspects of four new anthraquinone-based copper(II)complexes of the general formula [Cu(L^1)B] (1, 2) and [Cu(L^2)B] (3, 4) where L^1 = 2-((2-mercaptophenylimino)methyl)phenol, L^2 = 2-((2-mercaptophenylimino)methyl)-4,6-di-tert-butylphenol and B are 1,10-phenanthroline,dipyrido[3,2-d:2',3'-f]quinoxaline-8,9-napthaquinone, in modulating in vitro photo-dynamic activities. Nucleus targeting complexes have shown remarkable cytotoxicity in visible-light to cancer cells (IC_{50} ~ 2-11 μM) with reduced dark toxicity (IC_{50}>50 μM) unlike other copper (II) complexes. Singlet oxygen generated on photo-sensitization of the complexes was the key cytotoxic species responsible for apoptotic damage of cancer cells. Degree of photo-cytotoxicity of the photo-activated complexes was related to the extent of $^1O_2$ generation which was probed by several photo-physical studies along with TD-DFT calculations. Presence of low-lying, long-lived triplet excited state and hence increased ability to generate $^1O_2$ from $^3O_2$ through type-II photo-process was proposed to explain the degree of photo-cytotoxicity of the complexes. We observed dual photo-sensitization of S-coordination and anthraquinone moiety for the complex **4** leading to remarkable PDT effect to cancer cells with minimal dark toxicity. Overall, our investigations on exploring the structural aspects of copper (II) complexes for PDT were a phenomenal break-through in developing copper-based photo-chemotherapeutics in the clinical arena of cancer therapy.

1. Introduction

Photodynamic therapy (PDT) has emerged as tumor specific and non-invasive treatment modality for cancer[1-3]. It requires simultaneous presence of photosensitizer (PS), non-toxic red light and molecular oxygen ($^3O_2$) to show anticancer activity. The excited triplet state of the PS transfers its energy to triplet molecular oxygen ($^3O_2$) and converts it into toxic singlet molecular oxygen ($^1O_2$) which oxidizes key cellular macromolecules like proteins, DNA [4]. Photofrin® is FDA approved first generation PDT drug which is the oligomeric mixture of porphyrin derivative and clinically tested against primarily esophageal cancer [5-6]. Although other porphyrins, phthalocyanines or their metal analogues absorbing red light have emerged as second and third generation PDT agents [7-10]. PDT is limited by severe hepatotoxicity, prolonged skin photo-sensitivity and other side effects related to the tumor non-specificity of the present drugs [6]. Photo-activated transition metal complexes absorbing longer wavelength light and exhibiting ligand exchange, intramolecular redox reaction, facile ligand release, generation of radical species including ROS (reactive oxygen species) on photo-activation, may be of particular interest in developing metal-based photochemotherapeutic agents [11-14]. However, high energy requirement (<500 nm) for activation as well as heavy metal toxicity related to the complexes of later transition metals are the major challenges for their application in clinical arena of photo-chemotherapy. On contrary, bio-essential and kinetically labile first-row transition metal complexes absorbing light in PDT window (600-800 nm) are however preferable for photo-chemotherapeutic applications in considering deeper tissue penetration of longer wavelength light[15-17]. Photo-labile complexes of vanadium, manganese, iron or cobalt are explored extensively for photo-activated chemotherapy in PDT window to various cancer cell lines [18-23]. Biologically benign copper (II) complexes absorbing lights (>600 nm) were also previously studied for photo-cytotoxicity to various cancer cells with significantly low IC_{50}values [24-29]. Significantly high dark-toxicity of the copper(II) complexes is the major hindrance in designing copper(II)-based PDT agents (Scheme S1, Table S1).

Facile redox activity of the copper(II) complexes by intracellular thiols could be responsible for increased dark-toxicity.

The anthracycline antibiotics like daunorubicin, doxorubicin and others are used as anticancer agents for past few decades. Such anthracycline drugs having planar anthraquinone moiety target telomeres to exhibit anti-proliferative activity [30-32]. Ability of photo-sensitized anthraquinone moiety in generating reactive oxygen species (ROS: $O_2^{\bullet-}$, $^1O_2$) [33] has prompted us to synthesize anthraquinone-based copper(II) complexes to modulate in vitro photo-cytotoxicity(Scheme 1). Here in, we report the synthesis, analytical characterization, photo-physical studies and theoretical evaluation of singlet oxygen generation ($^1O_2$) on photo-activation, nuclear localization, cytotoxicity studies in MCF-7 and HaCaT cells in dark and visible light (400-700 nm, 10 Jcm^{-2}) of four new ternary copper(II)complexes of following formulas [Cu(L^1)B] (**1-2**) and [Cu(L^2)B] (**3-4**), where L^1 = 2-(2-mercaptophenylimino)methyl)phenol, L^2 = 2-(2-mercaptophenylimino)methyl)-4,6-di-tert-butylphenol and B= 1,10-phenanthroline (L^3) and anthraquinyl-dipyridoquinoxaline (L^4)(Scheme 1).

.

2. Experimental Section

2.1. Materials and Reagents

The reagents and all chemicals were obtained from Sigma-Aldrich (USA), SD-Fine chemicals (India), HI-MEDIA and used as received without any further purification. The solvents used were purified by standard methods [34]. DCFH-DA, Propidium iodide (PI), diphenylisobenzofuran (DBPF), Annexin V-FITC/PI was purchased from Sigma-Aldrich (USA). 1, 10-phenanthroline monohydrate (A.R.), Potassium bromide (KBr), 3,5-ditertbutyl-2-hydroxybenzaldehyde, 2-Aminothiophenol, 1,2-diaminoanthraquinone. A previously reported synthetic procedure was used to synthesize 1,10-phenanthroline-5,6-dione,Salicylideneimine-2-thiophenol(satpH2), 2((2mercaptophenylimino)methyl)4,6-ditertbutylphenol and 10,11[1,4naphthalendione]dipyrido[3,2-a;2”,3”-c]phenazine(Aqphen) with minor modification[35-38].

FT-IR spectra were recorded in solid phase using Perkin-Elmer UATR TWO FT-IR Spectrometer operating from 400 to 4000 cm^{-1}, UV-vis and emission spectra were recorded on Perkin-Elmer UV/VIS spectrometer and HITACHI F-7000 Fluorescence spectrophotometer respectively. Time-correlated single-photon-counting (TCSPC) spectrometer (Horiba Jobin Yovon) was used to accomplish fluorescence lifetime measurement. Nanosecond laser of 375 nm was used as excitation source in the following decay kinetics. The data were analysed by a bi-exponential fitting program using IBH DAS-6 decay analysis software. Molar conductivity measurements were done by using a EUTECH INSTRUMENT CON 510 (India) conductivity meter. Cyclic voltammetry of the complex (**1-4)** in DMF was studied at 25^0C using a EG & G PAR 253 Versa Stat potentiostat/galvanostat with a three electrode configuration consisting of a glassy carbon working, a platinum wire auxiliary and a saturated calomel reference (SCE) electrode. Ferrocene ($E_{1/2}$ =0.42 V) was used as a standard in MeCN 0.1 M $[nBu_4N](ClO_4)$ (TBAP) .

2.2. Synthesis

All the ligands (L^1, L^2 and L^4) were synthesized according to the literature [35-38] and further verified by Q-TOF ESI mass spectroscopy.

General synthesis procedure for L^1–L^4:

Salicylideneimine-2-thiophenol (**L^1**): A mixture of salicylaldehyde (5 mL, 47.8 mmol), o-aminothiophenol (4.696ml, 47.8 mmol) were heated to 80^0C and refluxed in 30 mL ethanol for 4 h. The reaction mixture was cooled to room temperature and the solvent was evaporated in vacuum and the resulting solid was recrystalized in ethanol. The yellow crystals were filtered and dried in air (Yield: ~80%, M.P: -130^0C)[35].

2-((2-mercaptophenylimino)methyl)4,6-ditertbutylphenol (**L^2**): A solution of 3,5-di-tert-butyl-2-hydroxybenzaldehyde (0.586g, 2.5 mmol) in benzene (30 mL) was added to a solution of 2-aminothiophenol (0.26ml, 2.5 mmol) in benzene (20 mL) and were heated at 100 °C in closed container under N_2 atmosphere for 3 days. The solvent was removed in vacuum. The product was obtained as yellow oil in a good yield (~80%) [36].

10,11-[1,4-naphthalendione]dipyrido[3,2-a;2",3"-c]phenazine (**L^4**): To the mixture of 1,10-phenanthroline (2.0 g, 0.011 mol) and KBr (2.00 g, 0.084 mol), H_2SO_4 (40 mL) followed by HNO_3 (20 mL) were added drop wise at 0°C. The resulting mixture was heated at 100°C until the bromine vapours disappeared. The solution was poured carefully into ice and slowly neutralized to pH 7.0 with 1M NaOH solution. The product was extracted with dichloromethane and dried over Na_2SO_4. The solvent was evaporated to get a yellow solid which was dried under vacuum to get yellow powder product1, 10–phenanthroline-5, 6-dione. (Yield: 1.96 g, 85%). M.P: 255-260 ^{0}C [37]. Mixture of 0.13g (1.24 mmol) of 1, 10-phenanthroline-5, 6-dione and 0.14g (1.24 mmol) of 1, 2-diaminoanthraquinone was refluxed in 30 ml ethanol at 85°C for 9 hours. After evaporating the ethanol, the suspension was filtered, and the dark brown residue was dissolved in 500 ml of hot chloroform in the presence of charcoal. Then, the orange coloured solution was concentrated to approximately 50 ml to obtain yellow solid. Diethyl ether was added to complete the precipitation. The product was filtered and dried under high vacuum to give golden yellow solid. (Yield: ~60%)[38].

The product was characterized spectroscopically and used for further complexation.

General synthesis procedure for preparation of the complexes (1-4):

Complexes (1-4) were prepared by a general procedure in which 0.199 g (1 mmol) quantity of monomeric copper(II) acetate monohydrate in 10 mL of MeOH was added with the respective Schiff bases [0.252g, 1.0 mmol of salicylideneimine-2-thiophenol (L^1) (**1** and **2**); 0.375 g of 2-((2-mercaptophenylimino)methyl)4,6-ditertbutylphenol (L^2) (**3** and **4**)] in 10 mL of MeOH while stirring at 25 °C for 1 h followed by addition of heterocyclic bases [0.162g, 1.0 mmol of 1,10-phenanthroline (L^3) (**1** and **3**); 0.371 g, 1 mmol of 10,11-[1,4-naphthalendione]dipyrido[3,2-a;2",3"-c]phenazine (L^4) (**2** and **4**)]. The mixture turned from blue to bluish green color. After being stirred for 2 h, the complexes were isolated as bluish green microcrystalline precipitate and washed with cold methanol, and finally recrystallization from MeOH into pale green colored microcrystalline solid. Yield: 0.392 g, 59% (**1**); 0.381 g, 52% (**2**), 0.429 g, 60% (**3**) and 0.451g, 56% (**4**).

Anal. Calc. For $C_{25}H_{19}N_3O_2SCu$ (**1**): Calculated: C, 63.75; H, 3.64; N, 8.92; Found: C, 63.17; H, 3.55; N, 8.99; FT-IR (Solid phase; br, broad; vs, very strong; s, strong; m, medium; w, weak)cm^{-1}: 2993m(NH), 1590m(C=N), 1210m, 830m, 721m, 617m, 521m(Cu-N), 495m(Cu-O), 425w(Cu-S).ESI-MS in CH_3CN: m/z 470.0361 $[Cu(L^1)(L^3)H]^+$. UV-visible in 10% v/v DMSO-H_2O [λ_{max}/nm (ε/L mol^{-1} cm^{-1})]: 265(2851), 394(127), 660(67),(sh, shoulder). Λ_M(Sm^2mol^{-1}) in 10% v/v DMSO-H_2O: 28 at 298 K.

Anal. Calc. for $C_{39}H_{21}N_5O_3SCu$ (**2**):Calculated: C, 66.61; H, 3.01; N, 9.96; Found: C, 65.97; H, 2.91; N, 9.92; FT-IR (Solid phase), cm^{-1}: 2995m(NH), 1575m(C=N), 1739s(C=O), 1328m, 1086m, 621m, 797m, 719s, 546w(Cu-N), 487m(Cu-O), 432w(Cu-S); ESI-MS in CH_3CN: m/z 702.0914 $[Cu(L^1)(L^4)H]^+$. UV-visible in 10% v/v DMSO-H_2O [λ_{max}/ nm (ε /L mol^{-1} cm^{-1})]: 274(1883), 404(945), 650(350); Λ_M(Sm^2 mol^{-1}) in 10% v/v DMSO-H_2O: 39 at 298 K.

Anal. Calc. For $C_{33}H_{33}N_3OSCu$ (**3**):Calculated: C, 67.96; H, 5.70; N, 7.20; Found: C, 67.51; H, 5.55; N, 7.11; FT-IR (Solid phase), cm^{-1}: 3006m (NH), 1614m (C=N),1210m, 755m, 683m, 537m(Cu-N),501(Cu-O), 445w(Cu-S).ESI-MS in CH_3CN: m/z 582.1640 $[Cu(L^2)(L^3)H]^+$. UV-visible in 10% v/v DMSO-H_2O [λ_{max}/ nm (ε/L mol^{-1} cm^{-1})]: 264(2654), 421 (212), 610(174), Λ_M(Sm^2 mol^{-1}) in 10% v/v DMSO-H_2O: 33 at 298 K.

Anal. Calc. for $C_{47}H_{37}N_5O_3SCu$ (**4**): Calculated: C, 69.23; H, 4.57; N, 8.59; Found: C, 69.13; H, 4.37; N, 8.51; FT-IR (Solid phase), cm^{-1}: 3011m (NH), 1618s (C=N), 1740s (C=O), 1262m,1170m, 859m, m, 719s, 530m(Cu-N), 492m(Cu-O), 436w(Cu-S). ESI-MS in CH_3CN: m/z 814.2688 $[Cu(L^2)(L^4)H]^+$. UV-visible in 10% v/v DMSO-H_2O [λ_{max}/ nm (ε/L mol^{-1} cm^{-1})]: 276 (3782), 397(971), 670(189). Λ_M(Sm^2 mol^{-1}) in 10% v/v DMSO-H_2O: 29 at 298 K.

3. Results and Discussion

3.1. Synthesis, characterization and general aspects

Complexes (**1-4**) were synthesized in 50-60% yield by a general synthetic procedure in which methanolic solution of $Cu(OAc)_2.H_2O$ was added with the Schiff base ligands (L^1 or L^2) pre-dissolved in MeOH followed by the addition of N,N-diimine ligands (L^3 and L^4) at room temperature with constant stirring for 2 h. Complexes were isolated as microcrystalline bluish-green precipitate and the pure solid was obtained after recrystallization from MeOH. Purity of the complexes were determined by elemental analysis (CHN analysis) and further characterized analytically and spectroscopically (Table S2). Non-conducting (Molar conductance, $\Lambda_{M,}$ 20-40 (Sm^2 mol^{-1}) in 10% v/v DMSO-H_2O) solution indicated as neutral complexes (Scheme 1)[29]. All the complexes were characterized by typical $C{=}N_{str}$ at ~1590-1620 cm^{-1} in addition to NH_{str} at ~2990-3010 cm^{-1} in solid-phase IR spectra. Moreover, $Cu\text{-}S_{str}$, $Cu\text{-}N_{str}$ were observed at ~420, ~550 cm^{-1} respectively in the solid-phase IR spectra of the complexes (Figure S1)[39]. Initially formation of the complexes was confirmed by the UV-visible spectral measurements recorded in 10% v/v DMSO-H_2O (Figure S2). Typical molecular ion peak for the complexes characterized by $[Cu(L)B]^+$ (L= L^1, L^2; B=L^3, L^4) was identified along with other fragmented mass in the Q-TOF ESI mass spectra (MS) of the complexes in acetonitrile (Figure S3-S6). Powder XRD spectrum of Cu(II) complexes are shown in Figure S7. Based on the data obtained analytically and spectroscopically we performed DFT calculations to obtain energetically favorable optimized structures and corresponding HOMO and LUMO stereographs are shown Figure S8.

3.2. Solubility and stability

Complexes (**1-4**) were soluble in acetonitrile (MeCN), methanol (MeOH), dimethylsulphoxide (DMSO), dimethylformamide (DMF), 5% v/v DMF-H_2O, 10% v/v DMSO-H_2O. Stability of the complexes on exposure to the visible light (400-700 nm, 10 Jcm^{-2}) was studied by UV-visible spectroscopy in which the complexes (1-4) in 10% v/v DMSO-H_2O (pH 6.8) were irradiated with visible light for 5 min followed by UV-Visible spectral measurements till 72 h (Figure S9). No apparent changes were observed in UV-Visible spectra of the complexes on visible light (400-700 nm, 10 Jcm^{-2}) exposure indicating the stability of the complexes on photo-exposure.

3.3. Electrochemical properties

Cyclic voltammetry of the complex **(1-4)** in DMF was studied at 25 ^{0}C using a EG & G PAR 253 Versa Stat potentiostat/galvanostat with a three electrode configuration consisting of a glassy carbon as working, a platinum wire as auxiliary and a saturated calomel as the reference (SCE) electrode. Ferrocene ($E_{1/2}$ = 0.42 V) was used as a standard in DMF containing 0.1 M [nBu_4N](ClO_4) (TBAP) (Figure S10). Complex **4** exhibited quasi-reversible cyclic voltammetric response with $E_{1/2}$ at -0.46 V and ΔE = 0.12V. The reduction potential for Cu(II)/Cu(I) system of the complex **4** was significantly higher beyond the biological redox window which is typically in the range +0.2 to -0.3 V. Such a high value of $E_{1/2}$ for complex **4** could be due to higher π accepting ability of the anthraquinyl moiety.

3.4. Electronic properties

Electronic spectra of the complexes (**1-4**) were recorded in 10% v/v DMSO-H_2O. Broad and weak metal-centered d-d band for the complexes were observed in the range 600-800 nm along with intense LMCT/MLCT bands at ~400 nm (Figure 1, Table S2). We observed red-shift in d-d band of the complex **3** and **4** clearly indicating the effect of strong electron donating t-butyl group on the electronic structure of the complexes. The nature of the electronic transitions and the MOs involved, obtained from TD-DFT calculations, are tabulated in (Table S3). The paramagnetic complexes **2** and **4** display typically poor luminescence in 400 and 518 nm under the similar experimental condition with luminescence quantum yield (φ, 0.04-0.05)(Table 1, Figure S11). Due to ^{3}IL emission of the anthraquinyl moiety, complex **4** has comparable luminescence which is also supported by spin density calculation.

3.5. Triplet excited state and luminescence life-time

Initially we probed the existence of low-lying triplet excited state of the complexes (**1-4**)[24]. Triplet-triplet annihilation (TTA) up-conversion generally requires a triplet photo-sensitizer for absorbing of the excitation energy and triplet acceptor for the up-converted emission. Energy is transferred from the

photosensitizer to the acceptor by triplet-triplet energy transfer (TTET) process followed by the singlet excited state of the acceptor is produced and the emission intensity of the acceptor is increased [40-44]. Typical increase emission spectrum of triplet perylene in MeCN was observed on photo-exposure in the presence of the complexes (**3**, **4**) (Figure S12). We assumed that photo-activated complexes quickly relaxed into the low-lying triplet excited state which was quenched by perylene resulting in emissive triplet perylene. Negligible emission of perylene was observed in the presence of the complexes in dark. Higher emission intensity of triplet perylene in the presence of complex **4** indicated effective inter-system crossing into triplet excited state. Similar observation was made for the complexes **1** and **2** (Figure S13).

Later we determined the steady state luminescence life-time of the complexes (**2**,**4**) at ambient temperature in MeOH and the first order luminescence decay of the complexes gave the life-time in nano second scale (Figure S14, Table 1). Although luminescence ligands were extremely short-lived complexes (**2**,**4**) exhibited longer luminescence life-time i.e. 11.3 ns, and 11.7 ns respectively. Longer luminescence life-time of the complexes could be due to the presence of low-lying and relatively long-lived triplet excited state in the complexes **2** and **4**.

3.6. Singlet oxygen ($^1O_2$) generation

Singlet oxygen ($^1O_2$) as ROS can be evidenced from a UV-visible spectral titration experiment. We probed the generation of singlet oxygen ($^1O_2$) on photo-activation (Visible light, 400-700 nm, 10 Jcm^{-2}) by the complexes (**1**-**4**) by using diphenylisobenzofuran (DPBF) (Figure S15)[43-44]. We also have determined the quantum yield of $^1O_2$ generation by using Rose Bengal as a reference (Figure S16). UV-Visible spectral titration was carried out to record the change in absorbance (A_{417nm}) of DPBF (50 μM) at λ_{max}= 417 nm in DMF against visible-light exposure (400-700 nm, 10 J cm^{-2}) time in the presence of complexes (50 μM). Gradual decrease in A_{417nm} of DPBF indicated photo-induced generation of singlet oxygen from complexes (**1**-**4**). Several control experiments with DPBF alone and DPBF in the presence of the complexes in dark excluded any possibility artifact. Degree of singlet oxygen ($^1O_2$) generation by

the complexes was graphically represented by plotting the extent of decrease in absorbance of DPBF (A/A_0) against photo-exposure time (t/sec), where A was the absorbance of DPBF at particular time while A_0 was the absorbance of DPBF at t= 0 sec. We observed almost linear decrease of absorbance of DPBF with photo-exposure time and indicated photo-induced generation of $^1O_2$ from $^3O_2$ by the complex via type II photo-process. The observed slope was different for the complexes (**1**-**4**) and the plot qualitatively explained higher amount of singlet oxygen generation by the complex **4**.

We quantified the singlet oxygen generation from the photo-activated complexes by determining the quantum yield ($\Phi(^1O_2)$) for singlet oxygen generation in reference to Rose Bengal in DMSO at room temperature (Table 1) [27]. The singlet oxygen quantum yield was determined to be in the range 0.2-0.6 for the complexes (**1**-**4**). Complex **4** generating higher amount of singlet oxygen ($^1O_2$) with quantum yield of 0.6 could be potential for PDT applications.

3.7. TD-DFT calculations and singlet oxygen ($^1O_2$) generation

We performed TD-DFT calculations further to verify the type-II photo-process of the complexes as predicted in several photo-physical studies and to correlate comparative efficiency of singlet oxygen generation by the photo-activated complexes (**1**-**4**). Time-dependent density functional theory (TD-DFT) calculations on the excited state of Cu(II)complexes (**1**-**4**) were carried out by using unrestricted B3LYP density functional theory[45]. Gauss Sum program was used to calculate the contribution of percentage of metal and ligands character involve corresponding in the HOMOs and LUMOs[46].The excitation energies and oscillator strengths, as well as the excited state compositions for the two systems presented were studied extensively.

Assuming type-II photo-process, initially we examined the presence of lowest lying excited triplet state for all the complexes by carrying out self-consistent, unrestricted B3LYP calculations at both the ground-state geometry as well as geometrically optimized triplet excited state. The vertical excitation

energies of low-lying doublet and triplet states of the complexes (**1-4**) were presented in Table 2. The nature of the low-lying excited states was determined to be typically MLCT and ILCT type and corresponding HOMO had significantly metallic character while LUMO was localized in the ligands. Doublet excited (D_1) state, populated upon absorption of visible light ($D_0 \rightarrow D_1$), efficiently populated further the low-lying triplet excited state (T_1) *via* strong inter-system crossing. Energy difference between low-lying doublet excited and triplet excited states of complexes (**1-4**) were 0.63 eV, 0.35 eV, 0.89 eV and 0.19 eV (Table 2, Figure 2). Therefore, we predicted better and faster inter-system crossing for the complex **4** probing the effect of bulky t-butyl group and anthraquinyl moiety for effective intersystem crossing in the complex and explain the significantly higher singlet oxygen ($^1O_2$) quantum yield (0.62).

3.8. Cellular uptake and cellular localization

Green luminescence of the complexes (**1**, **4**) was explored to study the cellular incorporation in HaCaTcells. The remedial effect of a drug is often related with its cellular uptake [47]. Complex **1** and **4** showed some increase in the cellular uptake compared to their free ligands (L^3, L^4). This observation reveals a crucial role of the metal in transporting the photosensitizer into the cells. We had standardized the incubation time for in vitro studies before light irradiation by cellular incorporation assay by FACS (Figure 4). The studies revealed predominant incorporation of the complex in 4h of incubation. The shift in the band position of the complexes (**1**, **4**) in HaCaT cells clearly indicates that the complexes have a higher cellular uptake compared to their free ligands (L^3, L^4).

Co-localization experiments were done to measure the intracellular presence of complex **4**. Only complex **4** has been selected to determine the intracellular distribution pattern by confocal microscopy as the cellular incorporation of other complexes and ligands were comparatively lower upon 4h incubation. Nuclear localization was observed from the merged images of the complex **4** (15μM) when treated with 4′,6-diamidino-2-phenylindole (DAPI) as the nuclear staining dye after 4 h of incubation in

dark (Figure 5).The merged image of the complex **4** and with nucleus staining dye 4′, 6-diamidino-2-phenylindole (DAPI) revealed selective localization of the complex into the nucleus of the cell.

3.9. Cytotoxicity and photodynamic effect

The ability of mitochondrial dehydrogenases in the viable cells to cleave the tetrazolium rings of 3-(4,5-dimethylthiazol-2-yl)-2,5-diphenyltetrazolium bromide (MTT) into dark violet membrane impermeable crystals of formazan was explored to probe cytotoxicity of the complexes in vitro in MCF-7 (human breast carcinoma) and HaCaT(human keratinocyte)cell lines in the dark and visible light (400-700 nm, 10 Jcm^{-2}) (Table 3, Figure S17)[23,24]. Cells were initially incubated with the complexes (**1**-**4**) in dose dependent manner at 37^0C for 4 h in the dark followed by photo-irradiation with visible light (400-700 nm, 10 Jcm^{-2}) for 1 hour. IC_{50} values were determined from the non-regression analysis of the dose-response plot for the complexes (**1**-**4**) and are presented in Table 3. We observed remarkable effect of visible light (400-700 nm, 10 Jcm^{-2}) on the cytotoxicity of the complexes (**1**-**4**) to both MCF-7 and HaCaT cells with IC_{50} values in the range 2.5-11.5 μM (Figure 6). Effect of ligands (L^1-L^4) alone, $Cu(OAc)_2.H_2O$ or visible light (400-700 nm, 10 Jcm^{-2}) on cytotoxicity to MCF-7 or HaCaT cells was insignificant and this excluded any artefact related to the cytotoxicity data. Complex **4** bearing anthaquinyl ligand exhibited remarkable photo-cytotoxicity with IC_{50} value of 2.5 μM and we observed >19-fold enhancement in cytotoxicity in comparison to dark (IC_{50}>50 μM) in HaCaT cells (photo-cytotoxicity index). Dual photosensitizing ability of S-coordination and anthraquinyl ligands in copper (II)-bound form could be responsible for such remarkable photocytotoxicity. Photofrin®, FDA approved first generation PDT drug, however, exhibited photodynamic effect to HeLa cells with IC_{50} of 4.3 μM and photocytotoxicity index ~10.23 The relative order of photocytotoxicity of the complexes was 4>2>3>1 which was directly correlated to the singlet oxygen quantum yield of the complexes (**1**-**4**) (Table 1).We observed remarkably reduced dark toxicity of the complexes (**1**-**4**) unlike other copper (II) complexes in previous findings [24-28]. Dark-toxicity of the copper (II) complexes was related to the facile redox chemistry of the complexes in biological redox window. However, reduction potential of

the complex **4** (E1/2 = -0.46 V) is far beyond the biological redox window to inhibit reduction of copper (II) into copper (I) by cellular thiols and thereby not able to produce cytotoxic hydroxyl radical in dark [46]. Reduction potential of Cu(II)/Cu(I) couple in aqueous DMF was high enough for glutathione to reduce Cu(II) into Cu(I) of complex 4. This was confirmed by UV-visible spectral titration of the complex 4 in aqueous DMSO against increasing concentration of glutathione (Figure S18). This resulted in reducing the dark-toxicity and enhanced photocytotoxicity index >19.

3.10. In vitro ROS generation

Quantification of intracellular ROS ($^1O_2$) generation was probed in our present study by flow cytometric analysis (FACS) on HaCaT cancer cells using non-polar cell permeable 2′,7′-dichlorofluorescein diacetate (DCFH-DA) dye (Figure S19)[48].The dye after hydrolysis by the intracellular esterase, was converted into highly green fluorescent 2′,7′-dichlorofluorescein (DCF) (λ_{em} = 525 nm) on oxidation by intracellular ROS or ROS generated *in situ*, emitting green light. Degree of photocytotoxicity of the complexes (**1**-**4**) was due to their ability to generate singlet oxygen ($^1O_2$) on photosensitization. Increase or shift in the fluorescence intensity was the measure of ROS generation. A change in fluorescence intensity of the HaCaT cells treated with the complexes **1** and **4** (5 μM) upon visible light exposure (400-700 nm, 10 Jcm^{-2}, 1 h) compared to the HaCaT cell alone gave us the measure of intensity of ROS generation. Complexes showed enhancement in the fluorescence intensity of DCF upon light compared to dark. We observed negligible shift in the fluorescence intensity of DCF in HaCaT cells treated with the complex **4** in dark while greater shift in fluorescence band of DCF was observed for HaCaT cells treated with the complex **4** in visible light. The result predicted the photo-activated generation of $^1O_2$ as ROS in vitro as the key cytotoxic species.

3.11. Apoptosis

It was very important to explore the nature of ROS-induced cell death. Apoptosis is a programmed cell death and unlike necrosis, does not induce any host immune response and toxic effects to the surrounding normal tissues. Therefore, apoptosis is more desirable cell death process for clinical applications. We performed Annexin-V-FITC/PI assay using flow cytometry to characterize the cell death process (Figure 7, Figure S20). Annexin-V-FITC/PI assay is based on the ability of Annexin- V to bind to phosphatidylserine which is a marker of apoptosis when it is on the outer leaflet of the plasma membrane. The single positive population has cells that are in early apoptosis and double positive population has cells that are in late apoptosis with compromised cell membrane. When most active complex **4** (5μM) treated with HaCaT cells, it was observed that the 65% in late apoptotic in visible light and 21% in dark respectively [49].

4. Conclusions

Overall, we prepared four new anthraquinone-based copper (II) complexes to explore singlet oxygen ($^1O_2$) mediated in vitro photodynamic activity to HaCaT and MCF-7 cells. The complexes exhibited reduced dark toxicity (IC_{50}> 50 μM). We probed in vitro ROS generation on photo-activation of the complexes that was leading to late apoptosis in HaCaT cells. We focused on the structural aspects of the complexes in modulating the toxicity in dark and in visible light. Based on the results obtained by photo-physical studies and TD-DFT calculations for the photo-activated complexes, we predicted a type II photo-process leading to the generation of singlet oxygen ($^1O_2$) from $^3O_2$ by energy transfer. Presence of relatively low-lying, long-lived triplet excited states for the complexes led to facile energy transfer to triplet oxygen ($^3O_2$) to generate ($^1O_2$). Low energy gap (0.19 eV) between D_1 and T_1 facilitating faster intersystem crossing to sufficiently long-lived triplet excited state (T_1) (τ, 11.7 ns), efficient quenching of T_1 by $^3O_2$ to generate $^1O_2$ ($\Phi(^1O_2)$, 0.6) and remarkable photo-cytotoxicity (IC_{50}, 2.5 μM) has led the complex **4** is of paramount importance in developing next-generation copper(II)-based PDT agents.

Acknowledgements

We thank the Science and Engineering Research Board, Government of India, New Delhi for financial support [ECR-2016-000839/CS], Board of Research in Nuclear Science (BRNS), Govt. of India (37(2)/14/18/2017-BRNS) and NIT Manipur for providing infrastructure. We sincerely thank Prof. Akhil R. Chakravarty, IISc Bangalore for providing the facility of cellular studies. We thank Prof. Abhijit Saha, UGC-DAE Consortium for Scientific Research, Kolkata for measuring luminescent decay for the complexes. We also sincerely thank Mr. A. K. Srivastava for helping us to carry out cyclic voltammetric study.

Electronic supplementary information (ESI):

IR, Q-TOF ESI mass and luminescence spectra of complexes; IR, UV-visible, luminescence spectra of the complexes (**1**-**4**), cyclic-voltammetric plot; UV-visible spectral measurement using DPBF and Rose Bengal with complexes; Steady state luminescence decay for the complexes; ROS generation studies; cellular localization; Geometrically optimized structure of the complexes with HOMO-LUMO stereographs; Cell viability assay and MTT plots; Annexin-VFITC/PI assay; Table on. IC_{50} values of selected copper (II) complexes, selected UV–Vis energy transitions at the TD-DFT/B3LYP level, cytotoxicity of the complexes in HaCaT and MCF -7 cells.

References

1. (a) D.E.Dolmans, D.Fukumura and R.K. Jain, Nat. Rev. Cancer.3(2003) 380-387. (b) A. P. Castano, P. Mroz and M. R. Hamblin, Nat. Rev. Cancer.6(2006) 535–545.
2. **(a)**W. Fan, P. Huang and X. Chen, Chem. Soc. Rev. 45(2016) 6488–6519. (b) F. Heinemann, J. Karges, and G. Gasser, Acc. Chem. Res.50(2017) 2727–2736.
3. **(a)** J. P. Celli, B. Q. Spring, I. Rizvi, C. L. Evans, K. S. Samkoe, S. Verma, B. W. Pogue and T. Hasan, Chem. Rev.110(2010) 2795–2838. **(b)** J. D. Knoll, B. A. Albani and C. Turro, Acc. Chem. Res.48(2015) 2280–2287. (c) J. M. Dąbrowski and L. G. Arnaut, Photochem. Photobiol. Sci.14(2015) 1765–1780.

4. N. L. Oleinick, R. L. Morris and I. Belichenko, Photochem. Photobiol. Sci.1(2002) 1–21.
5. S. Bonnet, Dalt. Trans.47(2018) 10330–10343.
6. **(**a**)** M. Ochsner, J. Photochem. Photobiol. B Biol.32(1996) 3–9**. (**b**)** The data was obtained from FDA **(**Food and Drug Administration**)**, http**://**www**.**accessdata**.**fda**.**gov /drugsatfdadocs/label/2008/020451s019lbl**.**pdf
7. A. Ormond and H. Freeman, Material*s* (Basel).6(2013) 817–840.
8. J. Mao, Y. Zhang, J. Zhu, C. Zhang and Z. Guo, Chem. Commun. 8(2009) 908-910.
9. S. S. Lucky, K. C. Soo and Y. Zhang, Chem. Rev.115(2015) 1990–2042.
10. M. Ethirajan, Y. Chen, P. Joshi and R. K. Pandey, Chem. Soc. Rev.40(2011) 340–362.
11. **(**a**)**M. K. Raza, K. Mitra, A. Shettar, U. Basu, P. Kondaiah, A. R. Chakravarty, Dalton Trans. 45(2016) 13234-13243.(b) H. Ali and J. E. van Lier, Chem. Rev.99(1999) 2379–2450.
12. **(**a**)** I. Romero-Canelón and P. J. Sadler, Inorg. Chem.52 **(**2013) 12276–12291**. (**b**)**N**.J.** Farrer, L**.** Salassa and P**.** J**.** Sadler, Dalton. Trans**.** (2009) 10690-10701**. (c)** A. Garai, A. Gandhi, V. Ramu,M. K. Raza, P. Kondaiah, A. R Chakravarty,ACS Omega3(2018) 9333-9338.
13. (a) L. B. Josefsen and R. W. Boyle, Met.-Based Drugs. 2008(2008) 276109. (b) B. Bertrand, K. Passador, C. Goze, F. Denat, E. Bodio and M. Salmain, Coord. Chem. Rev.358(2018) 108–124.
14. U.Schatzschneider, Eur. J. Inorg. Chem.2010(2010)1451–1467**.**
15. A**.**R**.** Chakravarty and M**.** Roy, Prog**.** Inorg**.** Chem**.**57**(**2012) 119-202.
16. K. Szaciłowski, W. Macyk, A. Drzewiecka-Matuszek, M. Brindell and G. Stochel, Chem. Rev.105(2005) 2647–2694.
17. U. Bhattacharyya, B. Kumar, A. Garai, A. Bhattacharyya, A. Kumar, S. Banerjee, P. Kondaiah, A. R. Chakravarty, Inorg. Chem.56**(**2017) 12457-12468.

18. (a) U. Basu, I. Khan, A. Hussain, P. Kondaiah and A. R. Chakravarty, Angew. Chemie - Int. Ed. 51(2012) 2658–2661**.** (b) A. Garai, I. Pant, S. Banerjee, B. Banik, P. Kondaiah, A. R. Chakravarty, Inorg. Chem.55(2017) 6027–6035.

19. (a) S. Banerjee and A. R. Chakravarty, Acc. Chem. Res.48(2015) 2075–2083. (b) S. Banerjee, A. Dixit, A. A. Karande and A. R. Chakravarty, Dalt. Trans.45(2016) 783–796.

20. S. B. Chanu, S. Banerjee and M. Roy, Eur. J. Med. Chem.125 (2017) 816–824**.**

21. A. K. Renfrew, E. S. O'Neill, T. W. Hambley and E. J. New, Coord. Chem. Rev. 2017. (doi.org/10.1016/j.ccr.2017.11.027).

22. A. K. Renfrew, N. S. Bryce and T. W. Hambley, Chem. Sci.4(2013) 3731–3739.

23. S. Saha, R. Majumdar, M. Roy, R. R. Dighe and A. R. Chakravarty, Inorg. Chem.48(2009) 2652–2663.

24. (a) D. Musib, M. K. Raza, S. Kundu and M. Roy, Eur**.** J**.** Inorg**.** Chem**.**2018(2018) 2011-2018. (b) D. Musib, S. Banerjee, A. Garai, U. Soraisam and M. Roy, ChemistrySelect.3(2018) 2767–2775.

25. (a) C. Al Hageh, M. Al Assaad, Z. El Masri, N. Samaan, M. El-Sibai, C. Khalil and R. S. Khnayzer, Dalt. Trans.47(2018) 4959–4967 (b) N. Mukherjee, S. Podder, S. Banerjee, S. Majumdar, D. Nandi and A. R. Chakravarty, Eur. J. Med. Chem.122(2016) 497–509. (c) N. Mukherjee, S. Podder, K. Mitra, S. Majumdar, D. Nandi and A. R. Chakravarty, Dalt. Trans. (2018) 823–835.

26. R.-K. Lin, C.-I. Chiu, C.-H. Hsu, Y.-J. Lai, P. Venkatesan, P.-H. Huang, P.-S. Lai and C.-C. Lin, Chem. Eur. J.24(2018) 4111–4120. (b) K. Laws, G. Bineva-Todd, A. Eskandari, C. Lu, N. O'Reilly and K. A. Suntharalingam, Angew. Chem. Int. Ed.57(2018) 287–29.

27. (a) A. Bhattacharyya, A. Dixit, S. Banerjee, B. Roy, A. Kumar, A. A. Karande and A. R. Chakravarty, RSC Adv.6(2016) 104474–104482**.** (b) R. Lin, C. Chiu, C. Hsu, Y. Lai, P. Venkatesan, P. Huang, P. Lai and C. Lin, Chem. Eur. J. 24(2018) 4111-4120. (c) D. V.

Belykh, A. S. Kozlov, Y. I. Pylina, I. S. Khudyaeva, A. S. Benditkis and A. A. Krasnovsky, Macroheterocycles. 12(2019) 68-74.

28. (a) T. K. Goswami, S. Gadadhar, M. Roy, M. Nethaji, A. A. Karande and A. R. Chakravarty, Organometallics. 31(2012)3010–3021**.** (b) T. K. Goswami, B. V. S. K. Chakravarthi, M. Roy, A. A. Karande and A. R. Chakravarty, Inorg. Chem. 50 (2011) 8452–8464. (c) B. Maity, M. Roy, B. Banik, R. Majumdar, R. R. Dighe and A. R. Chakravarty, Organometallics.29(2010)3632–3641.
29. I. Ali, W. A. Wani, K. Saleem,, Metal-Organic, and Nano-Metal Chemistry.43 (2013) 1162-1170.
30. E. M. Malik and C. E. Müller, Med. Res. Rev.36 (2016) 705-748.
31. X. Zhang, W. Zong, W. Cheng and X. Han, J. Met. Chem. B. 6 (2018) 5243-5247.
32. X. Qu, C. Wan, H. -C. Becker, D. Zhong and A. H. Zewail,Proc., Natl. Acad. Sci. U.S.A.98 (2001) 14212-14217.
33. S. C. N. Montoya, L. R. Comini, M. Sarmiento, C. Becerra, I Albesa, G. A. Argüello, J. L. Cabrera, J. Photochem. Photobiol. B: Biology.78(2005) 77-83.

34 D. D. Perrin, W. L. F. Armarego and D. R. Perrin, Purification of Laboratory Chemicals, Pergamon Press, Oxford, 1980.

35 (a) S. Durmus, B. M. Ates, O. Atakol, F. Ercan, and Z. Kristallogr.220 (2005) 973-976. (b) M. Aksu, S. Durmus, M.Sarı, K. C. Emregul, I. Svoboda, H. Fuess and O. Atakol, J. Therm. Anal. Calorim. 90 (2007) 541-547. (c) A. Soliman and G. G. Mohamed, Thermochim. Acta. 421(2004) 151-159.

36 (a) N. Dupont, Y.F. Ran, H.P. Jia, J. Grilj, J. Ding, S.X. Liu, S. Decurtins and A. Hauser,Inorg. Chem.50(2011) 3295-3303. (b) C. J. Moody, C. W. Rees and R. Thomas, Tetrahedron.48(1992) 3589-4628. (c) R. Lopez, B. Loeb, T. Boussie and T. J. Meyer, Tetrahedron Lett.37 (1996) 5437-5440.

37 (a) M. Steiner and A. Duerkop, Analyst.136(2011) 148-154. (b) D. M. Murphy, K. McNamara, P. Richardson, V. Sanchez-Romaguera , R. E. P. Winpenny and L. J. Yellowlees, Inorg. Chim. Acta.374(2011) 435-441.

38 A. Bhunia, S. Manna, S. Mistri, A. Paul, R. K. Manne, M. Kumar Santra, V. Bertolasi and S. C. Manna, RSC Adv. 5 (2015) 67727-67737.

39 K. Nakamoto, Infrared and Raman Spectra of Inorganic and Coordination Compounds: Part A: Theory and Applications in Inorganic Chemistry, 6th Ed., 2008, John Wiley & Sons, Inc.(ISBN: 9780471743392).

40 J. Sun, F. Zhong, X. Yi and J. Zhao, Inorg. Chem. 52 (2013) 6299–6310.

41 T. N. Singh-Rachford, F. N. Castellano, Coord. Chem Rev. 254(2010) 2560-2573.

42 J. Zhao, S. Ji and H. Guo, RSC Adv. 1(2011) 937-950.

43 W. Wu, J. Zhao, H. Guo, J. Sun, S. Ji and Z. Wang, Chem. - A Eur. J.18(2012)1961–1968.

44 J. E. Yarnell,A.Chakraborty,M. Myahkostupov,K. M. Wrightand F. N. Castellano, Dalton Trans.2018(doi:10.1039/C8DT02496K).

45 (a) M. J. Frisch, G. W. Trucks, H. B. Schlegel, G. E. Scuseria, M. A. Robb, J. R. Cheeseman, G. Scalmani, V. Barone, B. Mennucci, G. A. Petersson, H. Nakatsuji, M. Caricato, X. Li, H. P. Hratchian, A. F. Izmaylov, J. Bloino, G. Zheng, J. L. Sonnenberg, M. Hada, M. Ehara, K. Toyota, R. Fukuda, J. Hasegawa, M. Ishida, T. Nakajima, Y. Honda, O. Kitao, H. Nakai, T. Vreven, J. A. Montgomery Jr., J. E. Peralta, F. Ogliaro, M. Bearpark, J. J. Heyd, E. Brothers, K. N. Kudin, V. N. Staroverov, R. Kobayashi, J. Normand, K. Raghavachari, A. Rendell, J. C. Burant, S. S. Iyengar, J. Tomasi, M. Cossi, N. Rega, J. M. Millam, M. Klene, J. E. Knox, J.B. Cross, V. Bakken, C. Adamo, J. Jaramillo, R. Gomperts, R. E. Stratmann, O. Yazyev, A. J. Austin, R. Cammi, C. Pomelli, J. W. Ochterski, R. L. Martin, K. Morokuma, V. G. Zakrzewski, G. A. Voth, P. Salvador, J. J. Dannenberg, S. Dapprich, A. D. Daniels, O. Farkas, J. B. Foresman, J. V. Ortiz, J. Cioslowski, and D. J. Fox,Gaussian 09, 2009, Rev. A.02. Gaussian, Inc., Wallingford; D. D. Roy, A. K. Todd,

and M. M. John, Gauss View 5.0.8., 2009, Gaussian, Inc., Wallingford; A. D. Becke, J.Chem. Phy.98(1993) 5648. (b) *GaussView 5.0* (Gaussian Inc., Wallingford, CT, USA), 2009.

46 D. S. Sigman, A. Mazumdar and D. M. Perrin, Chem. Rev.93(1993) 2295-2316.

47 M. K.Raza,S. Gautam,P. Howlader,A. Bhattacharyya,P.Kondaiah,and A. R. Chakravarty,Inorg. Chem. 57(2018) 14374-14385.

48 (a) B. Ali, M. A. Iqbal, ChemistrySelect.2 (2017) 1586-1604. (b) L. B. Josefsen, R. W. Boyle, Met. Based Drugs. 154(2008) 1-3.

49 M. K. Raza, S. Gautam, A. Garai, K. Mitra, P. Kondaiah, A. R Chakravarty,Inorg. Chem. 56(2017) 11019-11029.

Table 1. Selected photophysical data for the complexes (**1**–**4**).

Complexes	**1**	**2**	**3**	**4**
λ_{ex}/nm (ε / $Lmol^{-1}cm^{-1}$)[a]	394(127), 660(67)	404(945), 650(350)	421(212), 610(174)	397(971), 670(189)
λ_{em} / nm[b]	452	443	400	518
Φ[c]	-	0.042	-	0.0562
$\Phi(^1O_2)$[d]	0.157	0.34	0.292	0.629
τ_L/RT(ns)[e]	-	11.3	-	11.7

[a]10% v/vH_2O-DMSO at 20 °C; [b]10% v/vH_2O-DMSO at 20 °C; [c]fluorescence quantum yields of the complexes in MeOH and anthracene (Φ_F, 0.27 in ethanol) as standard; [d]singlet oxygen quantum yield of the complexes with DPBF and Rose Bengal as standard in DMSO at 20 °C; [e]Luminescence lifetime of the complexes in MeOH at RT[λ_{ex} (laser), 375 nm].

Table2. Selected lowlying excited states, Calculated Energies **(**E**)**, and Dominant Orbital Excitation from TDDFT Calculations for all Cu**(**II**)** complexes lowlying doublet and triplet state Calculated at TDDFT/B3LYP/631G**(**d,p**)**/LanL2DZ level**.**

	State	Orbital excitation	Character	-E[a] (a.u)
1	T_1	HOMO3(β)-LUMO1(β)(97%)	MLCT	1408.4681
	D_1	HOMO1(β)-LUMO5(β)(28%)	MLCT	1408.4456
2	T_1	HOMO 4(β)-LUMO(β)(25%)	ILCT/MLCT	2279.3424
	D_1	HOMO1(β)-LUMO2(β)(96%)	MLCT	2279.3296
3	T_1	HOMO2(β)-LUMO2(β)(40%)	ILCT/MLCT	1722.9072
	D_1	HOMO(β)-LUMO3(β)(40%)	ILCT/MLCT	1722.8741
4	T_1	HOMO6(β)-LUMO(β)(31%)	ILCT	2517.1343
	D_1	HOMO2(β)-LUMO2(β)(46%)	MLCT	2517.1279

[a]The energy value corresponds to the absolute energy of the respective states.

Table 3. Cytotoxicity data (IC_{50}/μM) of the complexes in dark and on visible light exposure

Complexes	**HaCaT Cell line** IC_{50} / μM			**MCF-7 Cell line** IC_{50} / μM		
	Dark[a]	Light[b]	Photo-cytotoxicity index(PI)	Dark[a]	Light[b]	Photo-index(PI)
1	44.45 (±4.32)	7.56(±0.14)	5	26.81 (±2.16)	4.53 (±0.32)	5
2	>50.0	6.81(±0.21)	>7	33.15 (±1.18)	3.81 (±0.13)	10
3	>50.0	11.56(±0.35)	>4	36.43 (±4.27)	5.45 (±0.23)	6
4	>50.0	2.57(±0.30)	>19	>50.0	3.03 (±0.25)	>16
$Cu(OAc)_2.H_2O$	ND	ND		>50.0	>50.0	
L^3	ND	ND		>50.0	>50.0	
L^4	ND	ND		>50.0	>50.0	

[a]IC_{50} values correspond to 24 h incubation in dark. [b]IC_{50} values correspond to 4 h incubation in the dark followed by 1 h photo exposure to visible light (400-700 nm,10 J cm^{-2}, post incubation 19 h). ND: Not determined

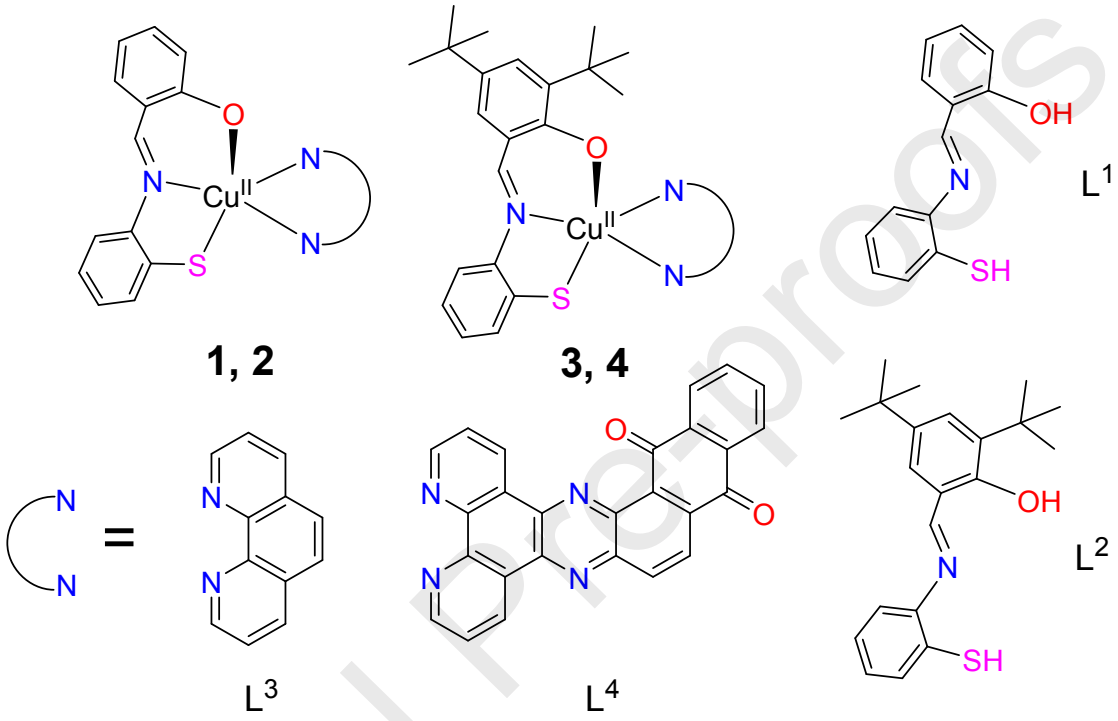

Scheme 1. Schematic representation of the complexes [Cu(L^1)B] (1-2) and [Cu(L^2)B] (3-4), where L^1 = 2-(2-mercaptophenylimino)methyl)phenol, L^2 = 2-(2- mercaptophenylimino)methyl)-4,6-di-tert-butylphenol and B= 1,10-phenanthroline (L^3) and anthraquinyl-dipyridoquinoxaline (L^4).

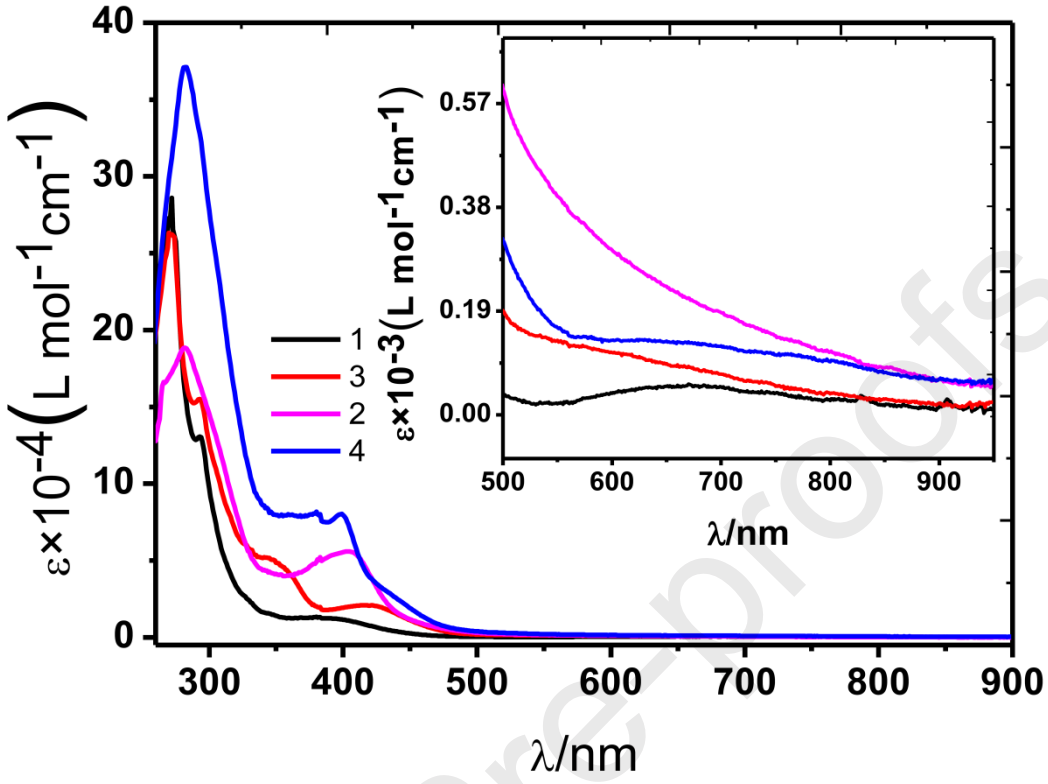

Figure 1. UV-visible spectra of the complexes **1** - **4** in 10% (v/v) H_2O-DMSO. Inset showed d-d bands.

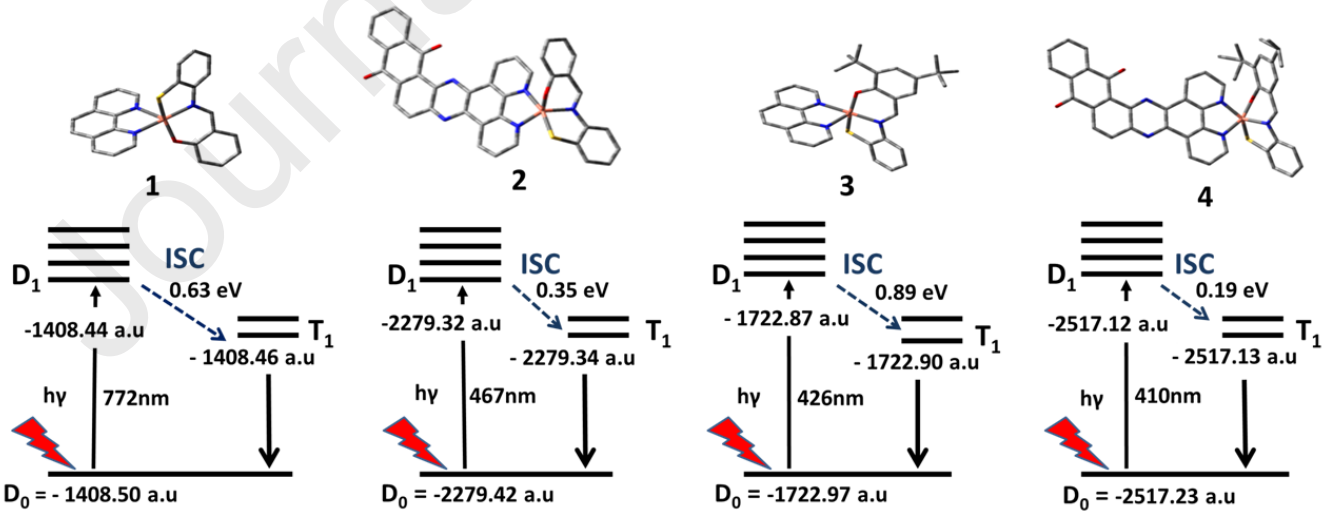

Figure 2. Schematic representation of type-II photo-processes in complexes (**1**-**4**).

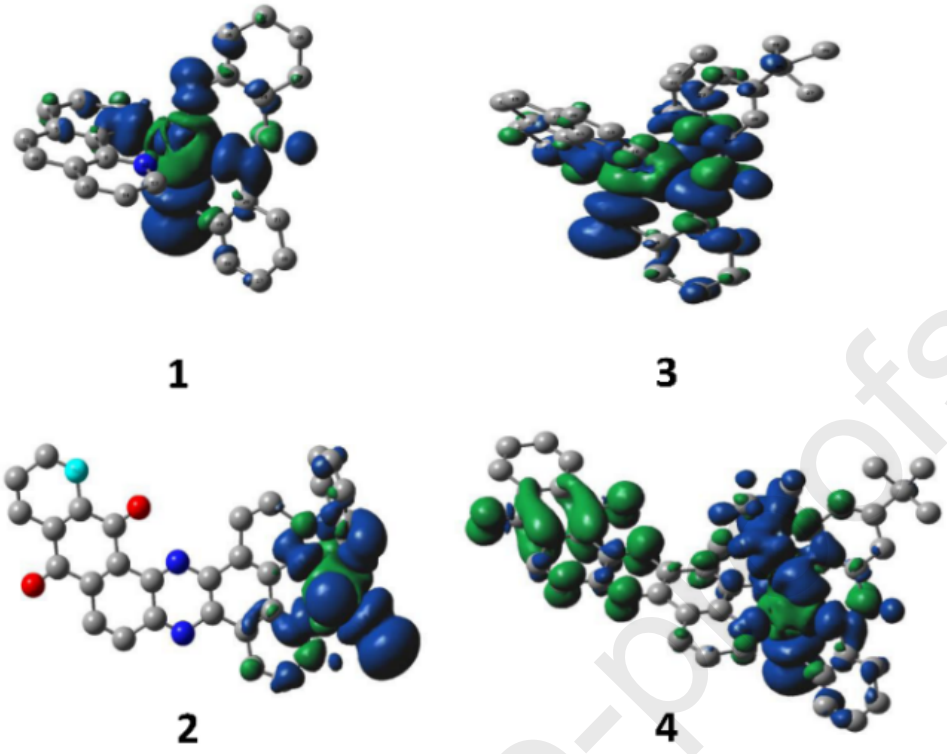

Figure 3. Isosurfaces of the spin density of the complexes (**1-4**) at the optimized T_1 excited-state geometry (isovalue ± 0.0004) calculated at the Calculated at TD-DFT//B3LYP/6-31G(d)/LanL2DZ level in gas phase with Gaussian 09W.

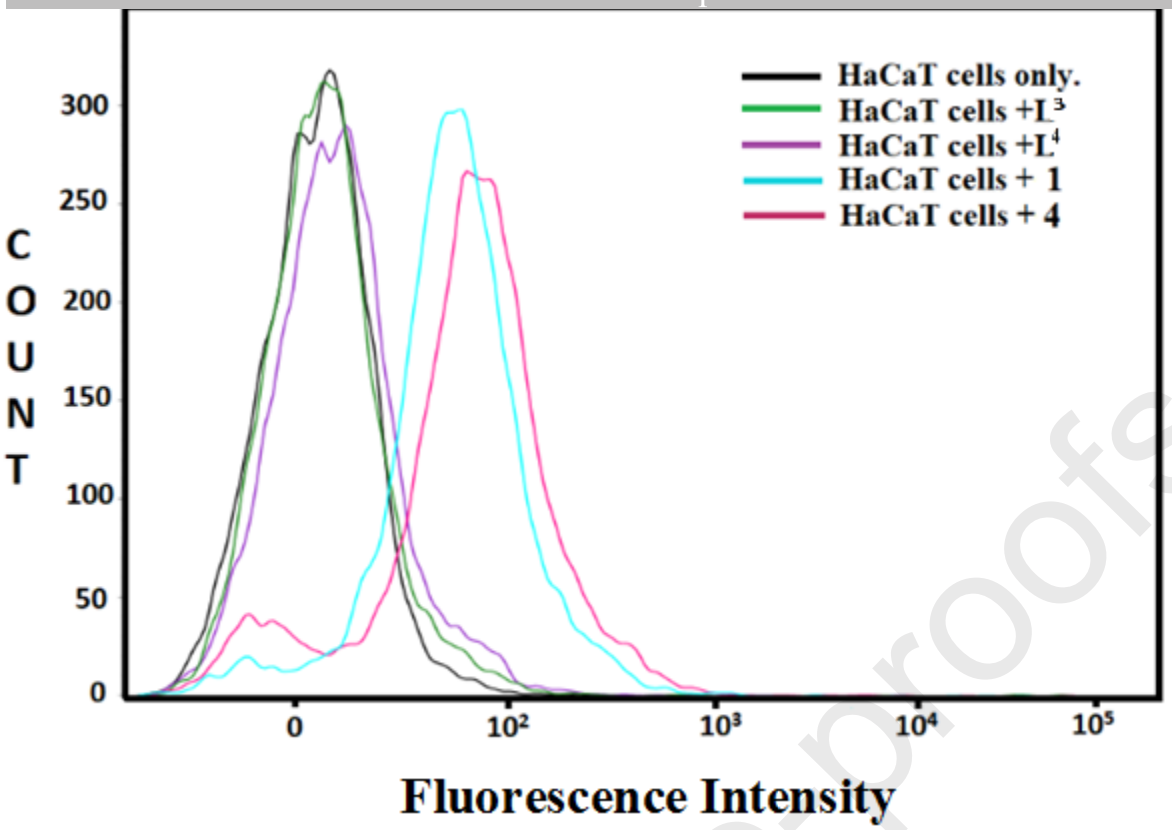

Figure 4. FACS analysis on quantitative cellular uptake of L^3, L^4 and complexes **1**, **4** in HaCaT cells, with cells untreated as a control. The shift in the band position of the complexes **1**, **4** in HaCaT cells indicates that the complexes have a higher cellular uptake compared to their free ligands L^3, L^4.Color legends are shown in the figure.

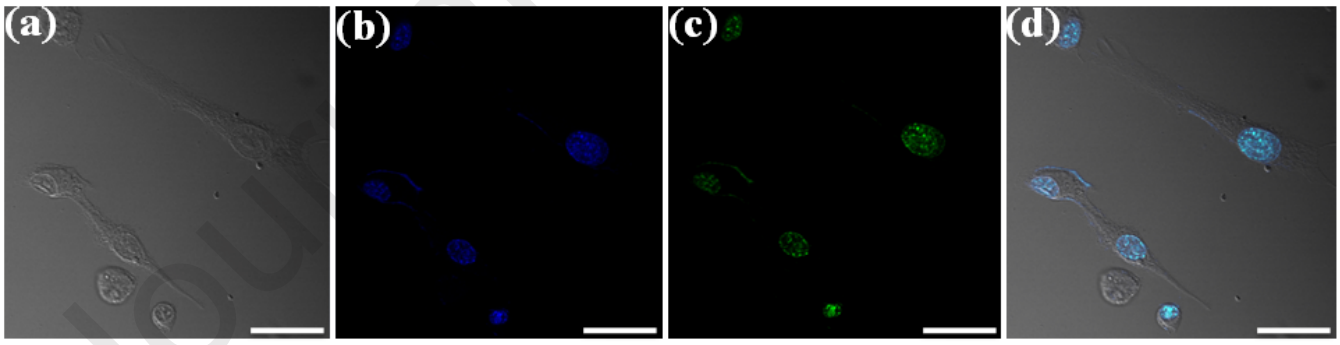

Figure 5. Confocal images of HaCaT cells. (a) Bright field images; (b) HaCaT cells stained with nuclear localizing dye (DAPI); (c) HaCaT cells treated with the complex **4** (15μM); (d) merged image indicating nuclear localization of complex **4**.

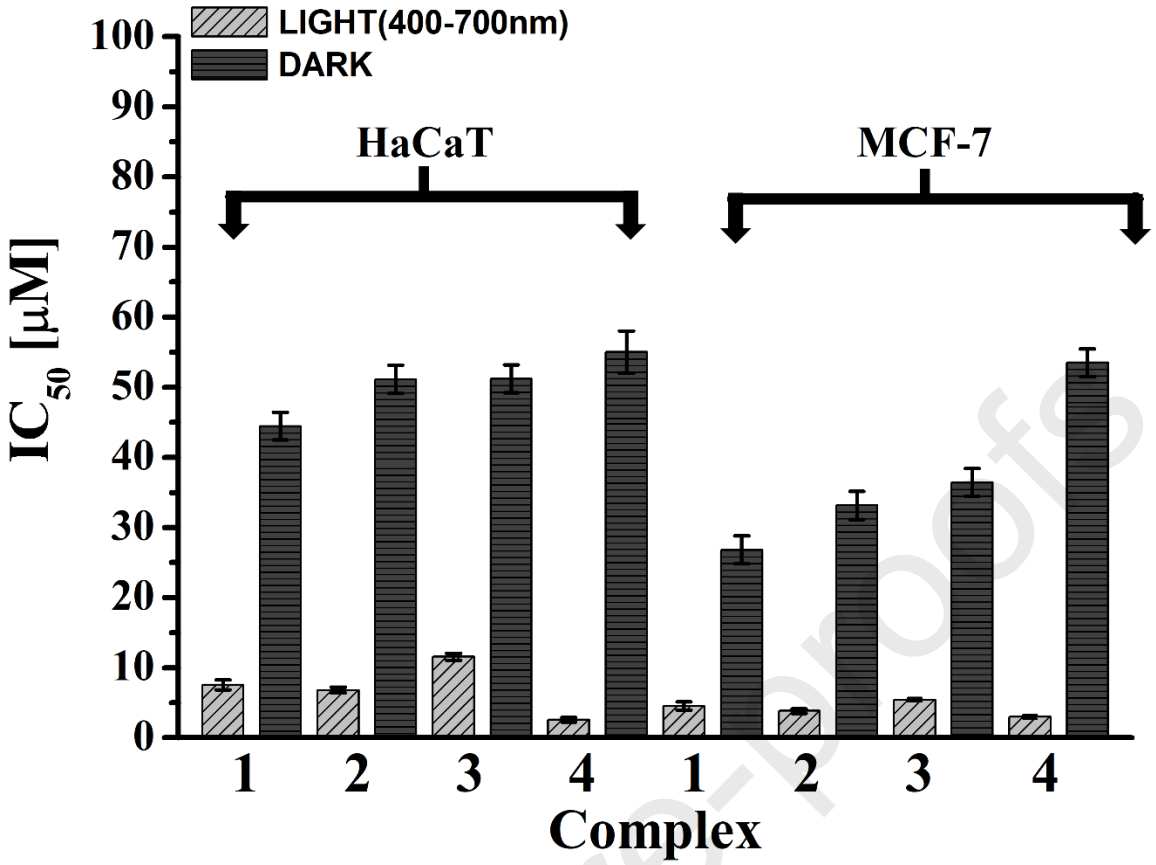

Figure 6. Bar diagram depicting the PDT effect of the complexes (**1**-**4**) in MCF-7 breast cancer and HaCaT skin keratinocyte cells in refrence to IC_{50} values determined from MTT assay [Visible Light: 400-700 nm, 10 Jcm^{-2}, Photo-irradiation Time: 1 h].

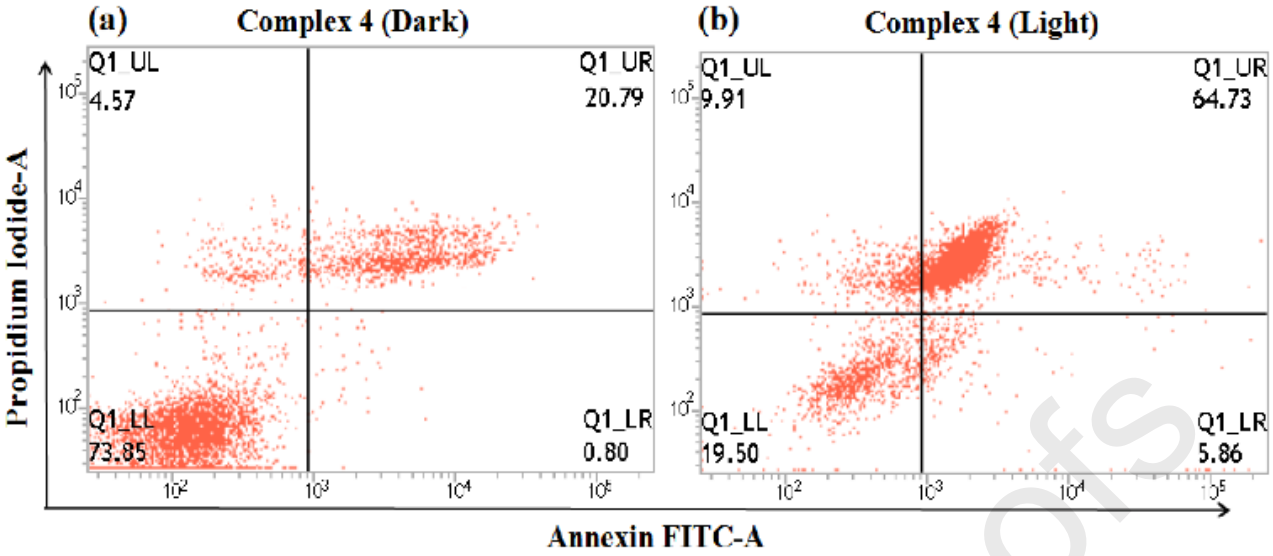

Figure 7. Annexin-V-FITC/PI assay showing the percent population of early apoptotic cells stained by annexin-V-FITC alone (lower right quadrant), dead cells stained by propidium iodide alone (upper left quadrant), or late apoptotic cells stained by both Annexin-V-FITC and PI (upper right quadrant) in HaCaT cells alone or treated with complex**4** in the dark (D) or after exposure to visible light (400− 700 nm, 10 Jcm^{-2}).

Nucleus targeting anthraquinone-based copper(II) complexes as the potent PDT agents: Synthesis, photo-physical and theoretical evaluation

Longjam Reena Devi,[†] Md Kausar Raza[‡], Vanitha Ramu[‡], Dulal Musib,[†], Joshila Devi[†] and Mithun Roy[*,†]

†Department of Chemistry, National Institute of Technology, Manipur, Langol 795004, Imphal (Manipur), India

‡Department of Inorganic and Physical Chemistry, Indian Institute of Science, Bangalore 560012 (India)

Synopsis: The present work explored structural aspects of copper (II) complexes for PDT of copper-based photo-chemotherapeutics. Nucleus targeting complexes have shown remarkable cytotoxicity in visible-light to HaCaT cells (IC_{50} ~ 2-11 μM) with significantly reduced dark toxicity (IC_{50}>50 μM) unlike other copper (II) complexes.

Table of Content Text: The present work explored nuclear localization; $^1O_2$ mediated *in vitro* photo-cytotoxicity with reduced dark toxicity of the anthraquinone-based copper (II) complexes.

Contents Fig.

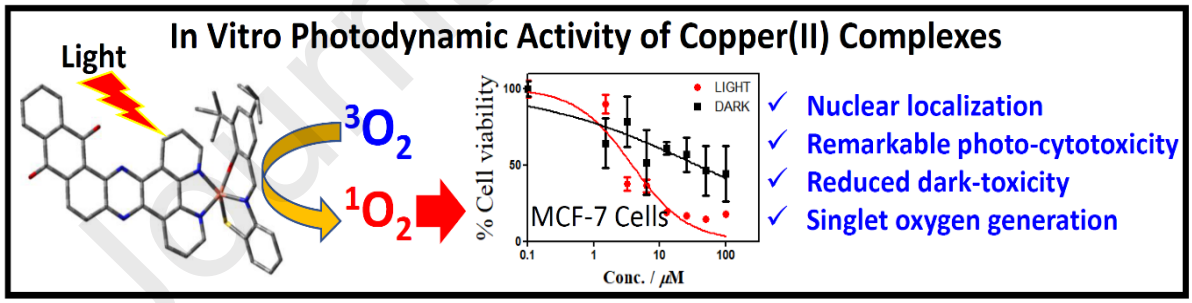

Highlights:

- *In vitro* photodynamic activity of anthraquinone-based copper(II) complexes is reported here.
- Increased concentration of singlet oxygen ($^1O_2$) generated from type-II photo-process was responsible for the photocytotoxicity through apoptosis.
- Generation of $^1O_2$ by the photo-activated copper(II) complexes was evaluated photo-physically and theoretically.